Effects of Interface on the Dynamic Mechanical Properties of PET/Nylon 6 Bicomponent Fibers

YOENG BAEG CHOI, SANG YONG KIM

Department of Fiber and Polymer Science, College of Engineering, Seoul National University, San 56-1, Shinlim-Dong, Kwanak-Ku, Seoul 151-742, South Korea

Received 25 February 1999; accepted 14 April 1999

ABSTRACT: Three types of drawn bicomponent fibers were investigated to find out the effects of interface on the crystallinity and the dynamic mechanical properties. They are in the form of side-by-side, alternating-radial, and island-sea types, and the core or island component is PET, and the sheath or sea component is nylon 6. From the results it is observed that the storage moduli of these fibers are higher and the maximum values of the loss tangent are lower than the values calculated by the Takayanagi parallel model. Also, the decrease of interfaces between the two components improves the crystallinity of the PET component in the bicomponent fibers compared with the single-component PET fiber. With the decrease in interfacial area, the maximum loss tangent decreases and the crystallinity increases at the same composition ratios. Among three types of bicomponent fibers, the side-by-side type—with the smallest interfacial area—has the highest crystallinity and the lowest maximum loss tangent.
 J Appl Polym Sci 74: 2083–2093, 1999

Key words: bicomponent fiber; PET; nylon 6; interface; dynamic mechanical

INTRODUCTION

The purpose of bicomponent fibers is to improve the material performance suitable for specific needs by tailoring one or more properties with minimum sacrifice of other properties. The behavior of bicomponent fibers can be said to depend on the behavior of each component in the bicomponent fibers, their relative composition ratios, and the nature of interfaces between the components.[1] In recent years, one of the most important use of the bicomponent fibers is "microfiber" for soft-touch fabrics, special cleaner, artificial leather, etc. The cross-sections of bicomponent fibers have been diversified to side-by-side, core-sheath, island-sea, matrix-fibril type, etc. For the finer touch of artificial leather or fabric, more complicated cross-sections of bicomponent fibers are in need nowadays. From this viewpoint, the shortcut to a successful bicomponent fibers is to attain adequate adhesion at the interface between two component polymers. Desirable bicomponent fibers usually combine two polymers so incompatibly that the filaments easily split at the stage of separation or extraction, but they must maintain the stable interface with good adhesion before the separation or extraction. The polyethylene terephthalate (PET)/nylon 6 bicomponent fibers are the most suitable combination corresponding to this desire.

Despite the large industrial activity in the bicomponent fibers,[2] there are very few papers on these fibers. But some studies about biconstituent fibers or polyblend fibers have been presented. According to the classification of incompatible polymer blend by Sperling,[3] the bicomponent and biconstituent fibers are different categories of crystalline polyblends. The bicomponent fibers

Correspondence to: Y. B. Choi.

Journal of Applied Polymer Science, Vol. 74, 2083–2093 (1999)
 CCC 0021-8995/99/082083-11

consist of two components divided into two relatively distinct regions within the cross-section extending along the length of the fiber. The biconstituent fibers, on the other hand, are composed of a more intimate blend in which one of the components consists of small, discrete fibrils embedded in a more or less continuous matrix. Thus, the research results on the behavior of biconstituent fibers appear not to be directly applied to the bicomponent fibers. Papero et al.[4] suggested that the nylon 6 fibrils act as nuclei for the formation of PET crystals in the interfaces of PET/nylon 6 biconstituent fiber, and the major constituents appear to crystallize more than the minor constituents, possibly reflecting some kind of physical interaction between the phases. Also, according to the results of Varma and Dhar,[5,6] the increased orientation of PET (fibril)/nylon 6 (matrix) biconstituent fiber was due to the highly oriented and extended PET chains holding the nylon 6 chains along their length, and the improvement of crystallinity and orientation was achieved due to the fibril-reinforced morphology and the crystallization behavior of the two components, especially that of nylon 6 in the presence of PET. Fakirov et al.[7] reported that during the long thermal treatment, in addition to the physical process (crystallization and relaxation), the chemical interactions (additional condensation and exchange reactions) take place at the interfaces in the drawn PET/nylon 6 blend systems, resulting in the formation of PET–polyamide 6 block copolymers.

The interfacial area of biconstituent fibers composed of two immiscible blends is about 10^0 to 10^2 m^2/g,[8] and it is approximately larger by one to four orders than the interfacial area of bicomponent fibers. In this study, the effects of interface on the dynamic mechanical properties of PET/nylon 6 bicomponent fibers have been investigated to obtain an understanding on the crystalline structure of the drawn PET/nylon 6 bicomponent fibers. To analyze the relationship between the interfaces and the crystalline structure, three types of bicomponent fibers with different magnitude of the interfacial area were used, and the dynamic mechanical properties of these fibers were compared with one another and the single-component PET and nylon 6 fibers.

EXPERIMENTAL

Bicomponent Spinning

Three types of bicomponent fibers were produced by extruding the melt of PET (IV 0.65, $\bar{M}_n \approx$ 25,000) as the core or island component and nylon 6 (RV 2.5, $\bar{M}_n \approx$ 21,000) as the sheath or sea component through three kinds of spinnerets using two different extrusion systems at the temperatures of 258°C for nylon 6 and 300°C for PET. Each extrusion system consists of an extruder and a metering pump. The combined melts with each cross-section type, i.e., side-by-side, alternating-radial and island-sea type, were extruded through 72 round holes of 0.23 mm diameter at 294°C. Figure 1 shows the three types of cross-sections of the bicomponent fibers used in this study, the bright portion in the cross-section being PET, and the other, nylon 6.

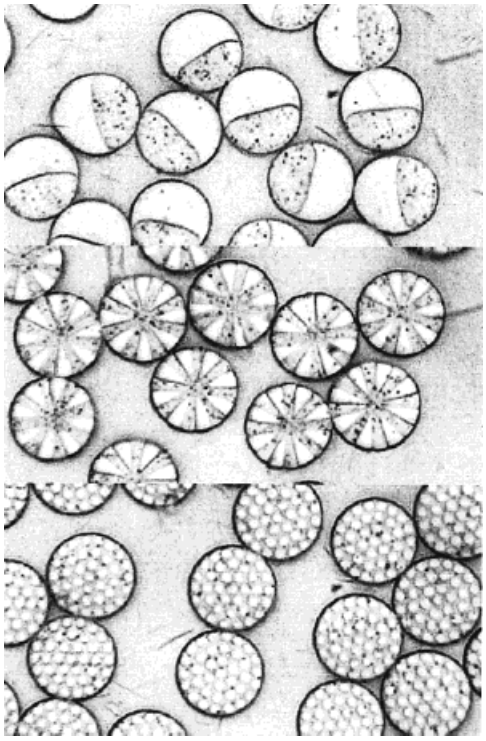

Figure 1 Fiber cross-section photographs of PET/nylon 6 bicomponent fibers at a composition ratio 55/45 vol %. The bright portion is the PET component; (a) side-by-side; (b) alternating-radial; (c) island-sea type cross-sections.

Six different mass flow rate combinations of PET/nylon 6 were used. The extruded bicomponent fibers were quenched and subsequently wound to yield the bicomponent POY (partially oriented yarn) fibers. Also, a single-component PET POY and nylon 6 POY were produced. Details are listed in Table I.

Drawing

The bicomponent POY fibers were drawn under a hot drawing conditions using a commercial draw

Table I Spinning and Drawing Variables of the PET/Nylon 6 Bicomponent Fibers and the Single Component Fibers

Spinning and Drawing Variables	Bicomponent Fibers	Single Component Fibers	
		PET	Nylon 6
Spinning temperature (°C)	294	293	264
Ratio of mass flow rate combinations of PET/nylon 6 (wt %)	30/70, 40/60, 50/50, 60/40, 70/30, 80/20	100/0	0/100
Take-up velocity (m/min)	3200	3200	3200
Draw ratio	1.53	1.53	1.23
Drawing temperature (°C)	80	80	20(r.t.)
Heat setting temperature (°C)	130	130	No
*Volume percent ratios of PET/nylon 6 compositions (vol %)	26/74, 36/64, 45/55, 55/45, 66/34, 77/23	100/0	0/100

* Volume percent ratios are converted from mass flow rate combinations of PET/nylon 6 (wt %).

twister. The single-component PET POY was drawn under the same hot drawing conditions, but the single-component nylon 6 POY was drawn in cold drawing conditions, which is in accordance with the general manufacturing practice. Details of drawing conditions are shown in Table I. Finally, 200 denier 72 filaments bicomponent fibers and two single-component fibers were produced.

Measurements

The temperature dependence of the storage modulus (E') and loss tangent (tan δ) of bicomponent fibers were measured at 110 Hz with a Rheovibron DDV-II, model RHEO-2000 (Orientec, Japan) at a temperature ranging from 30 to 200°C. The heating rate was 2°C/min. The sample length and the amplitude were 30 mm and ± 16 μm, respectively. The cross-sectional areas of the bicomponent fibers were determined from the deniers and the densities that were measured by a floatation method using *n*-heptane–carbon tetrachloride mixtures. The bicomponent fibers were cut with a microtome to produce its cross-section for the image processing. An electronic imaging program "Image-Pro Plus" programmed by Media Cybernetics was used with a built-in microscope to analyze the image of the cross-section and to calculate the interfacial area. Wide-angle X-ray diffraction patterns of the fibers were taken using the Ni-filtered CuKα radiation with an X-ray diffractometer, model RU-200B (Rigaku, Japan). The melting and crystallization behavior were examined using a Perkin-Elmer differential scanning calorimeter DSC-7 at a heating and cooling rate of 20°C/min. The sample weight was 9 to 10 mg. The temperature and heat of fusion were calibrated with indium and zinc.

RESULTS AND DISCUSSION

In the island-sea type bicomponent fibers, the number of PET islands are 37, and the alternating-radial type bicomponent fibers have eight PET segments. The photographs of three types of PET/nylon 6 bicomponent fibers are shown in Figure 1, at a composition ratio 55/45 vol %.

The storage modulus (E') vs. temperature curves of alternating-radial type bicomponent fibers are shown in Figure 2(a) and (b). In these figures, the solid lines are the experimental storage moduli of PET and nylon 6 single-component fibers, and the broken lines [Fig. 2(b)] are the calculated values by the Takayanagi parallel model shown in Figure 3. The calculation[9] is made by using Eq. (1) with the storage moduli of PET and nylon 6 single-component fibers:

$$E'_{\mathrm{B}} = \nu_{\mathrm{PET}} E'_{\mathrm{PET}} + \nu_{\mathrm{nylon\ 6}} E'_{\mathrm{nylon\ 6}} \qquad (1)$$

where E'_{B}, E'_{PET}, and $E'_{\mathrm{nylon\ 6}}$ are the storage moduli of bicomponent fibers, PET, and nylon 6 fiber, respectively, and υ_{PET} and $\upsilon_{\mathrm{nylon\ 6}}$ are the volume fractions of PET and nylon 6 component in the

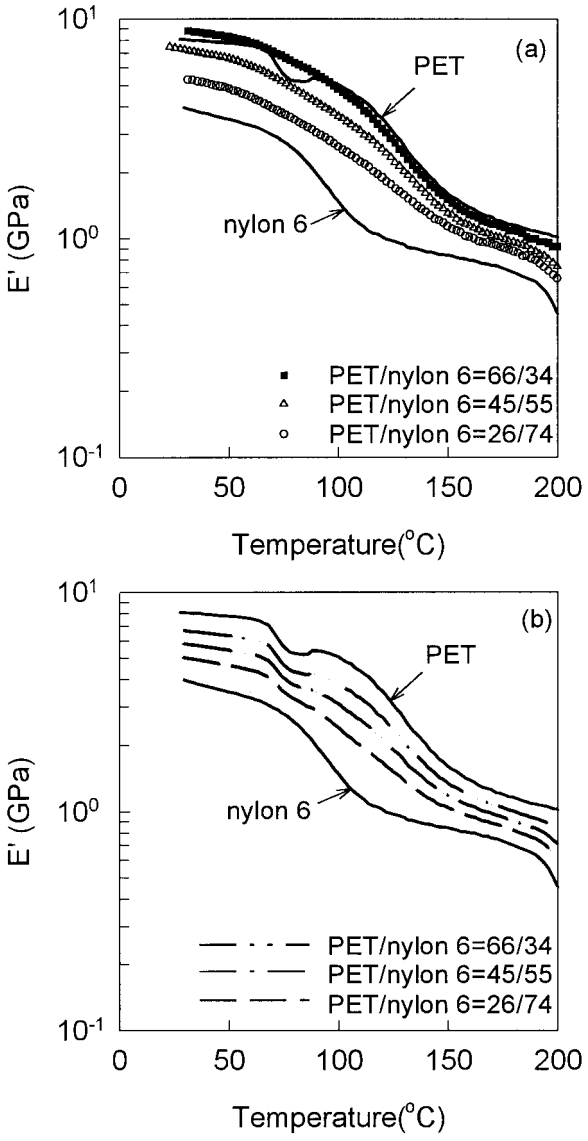

Figure 2 Storage moduli of alternating-radial type of the PET/nylon 6 bicomponent fibers at various composition ratios (vol %); (a) symbols: measured; (b) broken lines: calculated by the Takayanagi parallel model.

bicomponent fibers, respectively. The Takayanagi model assumes basically the different morphological structures in the blend or composite. In addition to this basic assumption, the Takayanagi parallel model assumes that both phases are continuous in space. Figure 3 demonstrates this model. A typical example is a continuous or long composite stretched in the fiber direction. The Takayanagi parallel model is an upperbound model, that is, no modulus higher than that derived from Eq. (1) is attainable.[10]

As shown in Figure 2(a) and (b), the storage modulus increases with the increase in the ratio of the PET component in the drawn alternating-radial type of the PET/nylon 6 bicomponent fibers. The experimental storage modulus curves [Fig. 2(a)] are in agreement with the calculated values [Fig. 2(b)] by the upperbound Takayanagi model. However, the experimental storage modulus values become gradually higher than the calculated with the increase in the ratio of PET component. At 66 vol % and the higher volume percent of PET component, the storage moduli of bicomponent fibers exceed the storage modulus of the PET single-component fiber. The increase of the storage modulus can be explained by the improvement of crystallization behavior of the systems. In the study of PET/nylon 6 biconstituent fiber, Varma and Dhar[5,6] suggested that the improvement of crystallinity and orientation of PET/nylon 6 (fibril/matrix) biconstituent fiber was achieved due to the fibril-reinforced morphology and the crystallization behavior of the two components, especially that of nylon 6 in the presence of PET. But, in the case of these bicomponent fibers composed with two incompatible polymers, it would not be possible to form the fibril-reinforced morphology. Thus, the higher storage modulus may be said to result from the effect of interface on the orientation-induced crystallization mechanism during the bicomponent fiber spinning and subsequent drawing processes. In Figure 2, the plateau, from 70 to 100°C, on the storage modulus curve of the PET fiber is assigned to the crystallization of the PET fiber,[11] and this

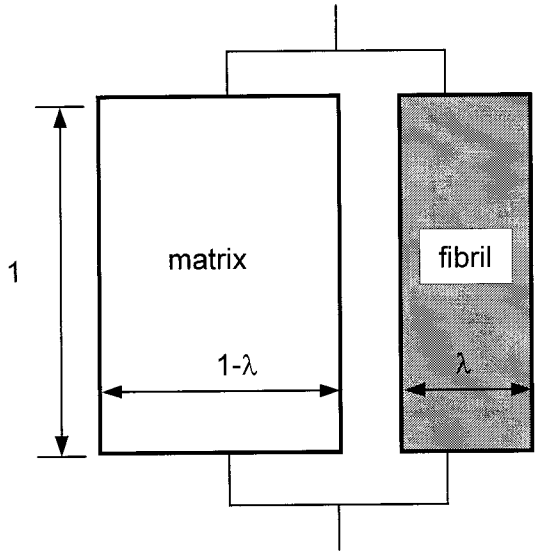

Figure 3 The Takayanagi parallel model for two-phase systems with fibril and matrix.

would be due to the insufficient drawing (draw ratio 1.53). The draw ratio 1.7 to 1.8 may be practically sufficient condition for PET POY that was wound with the take-up speed of 3200 m/min. Although the bicomponent fibers do not have the plateau of crystallization of the PET component at any composition ratios, this means that the crystalline structure of the PET component in the bicomponent fibers is well developed compared with the single-component PET fiber.

The loss tangent (tan δ) curves as a function of temperature of the drawn alternating-radial type PET/nylon 6 fibers are shown in Figure 4(a) and (b). The PET and nylon 6 single-component fibers show the maximum loss tangent peak around 100 and 134°C, respectively. The bicomponent fibers have two peaks of loss tangent corresponding to the peaks of two components. With the increase in the ratio of PET component in the bicomponent fibers, the peak at the low-temperature region decreases, whereas the peak at the high temperature region increases. At 66 vol % and the higher volume percent of the PET component, the peak at the low-temperature region disappears. It can be seen that the measured loss tangent values [Fig. 4(a)] are in good agreement with the calculated ones [Fig. 4(b)]. The calculation[9] is made by using Eq. (2) with the loss tangent of PET and nylon 6 single-component fibers:

$$\tan \delta_B = \frac{\tan \delta_{\mathrm{PET}} E'_{\mathrm{PET}} \nu_{\mathrm{PET}} + \tan \delta_{\mathrm{nylon\ 6}} E'_{\mathrm{nylon\ 6}} \nu_{\mathrm{nylon\ 6}}}{E'_{\mathrm{PET}} \nu_{\mathrm{PET}} + E'_{\mathrm{nylon\ 6}} \nu_{\mathrm{nylon\ 6}}} \quad (2)$$

where tan δ_B, tan δ_{PET}, and tan $\delta_{\mathrm{nylon\ 6}}$ are the loss tangent of the bicomponent fibers, PET, and nylon 6 fiber, respectively. However, the peaks of loss tangents at the high-temperature region are lower than the calculated ones with the increase in the ratio of the PET component. The peaks of loss tangent at the high-temperature region correspond to the α-relaxation peak of the PET component in the bicomponent fibers. Murayama[9] reported that the intensities of the loss tangent decrease with the increase in crystallinity. Thus, the decrease of the maximum loss tangent can be considered due to the higher crystallinity of the PET component. The loss tangent curves of three types of PET/nylon 6 bicomponent fibers at a composition ratio 66/34 vol % are shown in Figure 5. The bicomponent fibers have nearly the same

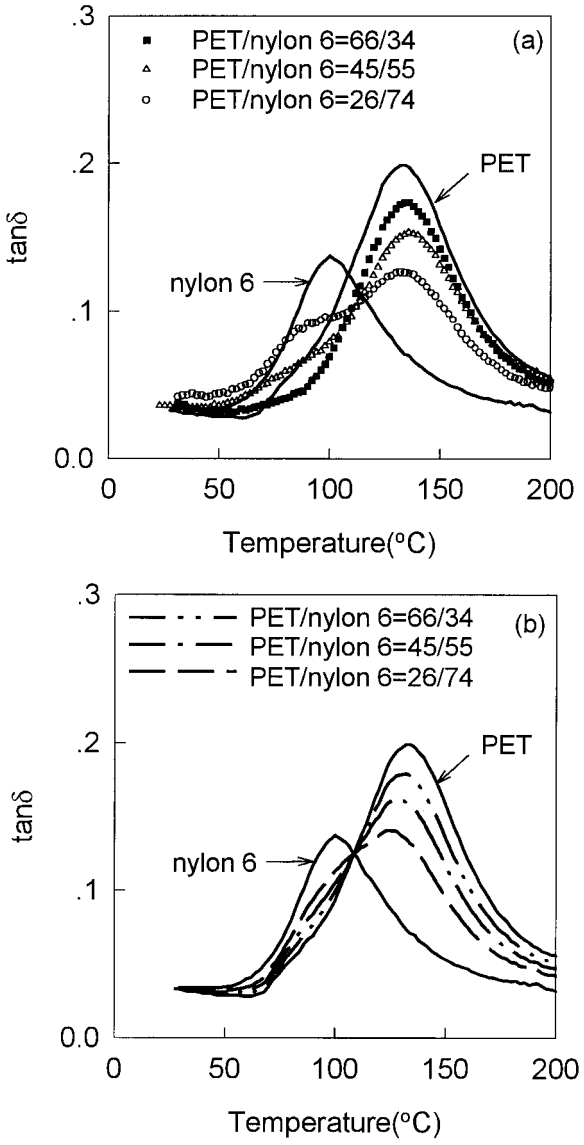

Figure 4 Loss tangent of alternating-radial type of the PET/nylon 6 bicomponent fibers at various composition ratios (vol %); (a) symbols: measured; (b) broken lines: calculated by Takayanagi parallel model.

peak temperatures, close to that of PET single-component fiber. The loss tangent and its maximum value of side-by-side type are lower than those of the other two types, as well as the calculated ones. The interfacial area of the three types of bicomponent fibers used in this study were estimated by the image processing and being 4×10^{-2} m^2/g to 8×10^{-1} m^2/g. Figure 6 shows that the interfacial area of alternating radial and island-sea types increase with the increase in the PET component, although that of the side-by-side type remains constant up to 45 vol % and then

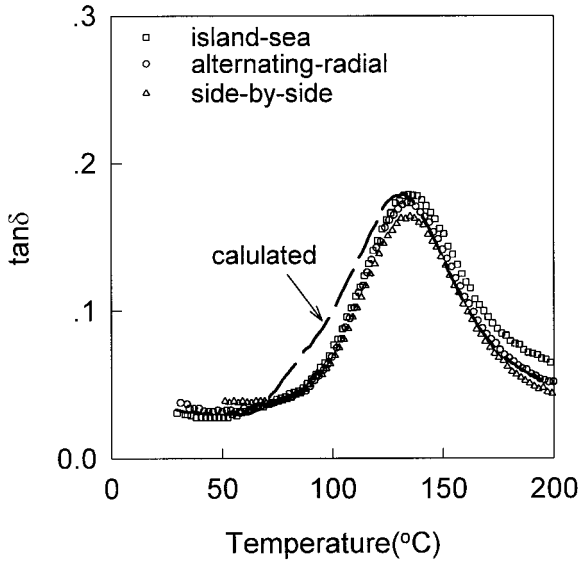

Figure 5 Loss tangent of the PET/nylon 6 bicomponent fibers at a composition ratio 66/34 vol %; dashed line: calculated by the Takayanagi parallel model.

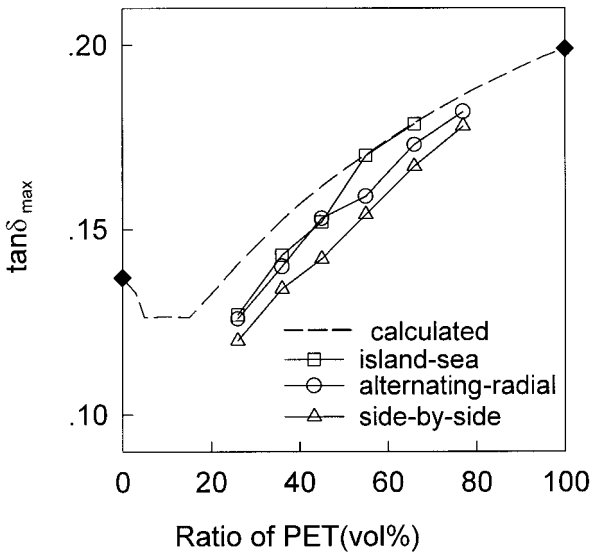

Figure 7 Maximum loss tangent of the drawn PET/nylon 6 bicomponent fibers; dashed line: calculated by the Takayanagi parallel model.

decreases with the increase in the PET component. Also, the side-by-side type has only one interface, as shown in Figure 1, and its magnitude is approximately smaller by 1/4 to 1/15 than those of other two types. Thus, it could be said that the relatively small interfacial area of the side-by-side type induces low maximum loss tangent.

As shown in Figure 7, the maximum loss tangent increases with an increase in the ratio of the PET component in all types of the bicomponent fibers. In the whole range of the PET composition ratio (26 to 77 vol %) of this study, the measured maximum loss tangent values of all types of the bicomponent fibers are lower than the calculated values. Obviously, Figure 7 shows that the maximum loss tangent decreases in the order of the interfacial area, i.e., from island-sea and alternating-radial types to the side-by-side type at the same composition ratios. Also, in Figure 8 it can be seen that the side-by-side type shows the higher maximum loss tangent temperature than those of other two types at the same composition ratios. Murayama[9] reported that in the case of PET with a low degree of crystallinity, the maximum loss tangent is shifted to the high-temperature region with an increase in crystallinity. Therefore, it can be explained that these trends of the temperatures and the peak values at the maximum loss tangents resulted from the increase of crystallinity, which may be due to the decrease of interfacial area. This explanation is in very good agreement with the dependence of the maximum loss tangent on the interfacial area, as shown in Figure 9. In this figure, it is known that the maximum loss tangent increases with the increase in the interfacial area in the bicomponent fibers.

These trends of the dynamic mechanical properties are good agreement with the weight percent crystallinity of the bicomponent fibers by DSC measurement (X_{DSC_B}), as shown in Figure

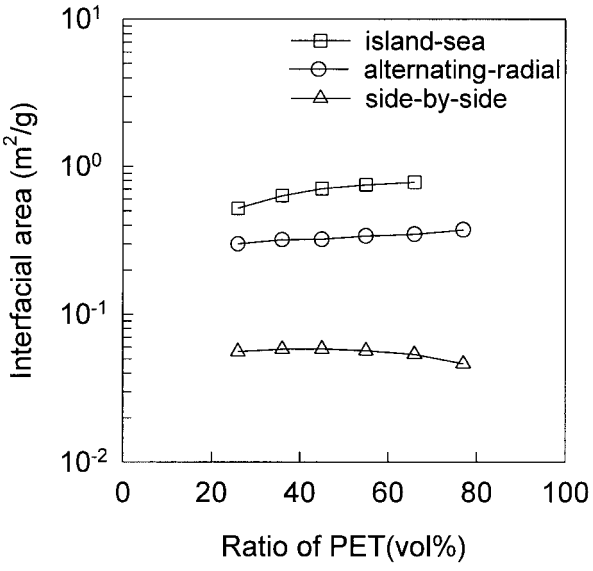

Figure 6 Interfacial area of the drawn PET/nylon 6 bicomponent fibers.

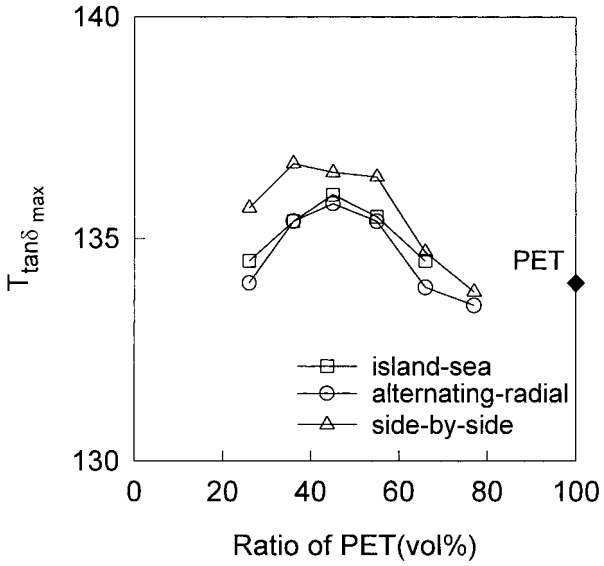

Figure 8 Maximum loss tangent temperature of the drawn PET/nylon 6 bicomponent fibers.

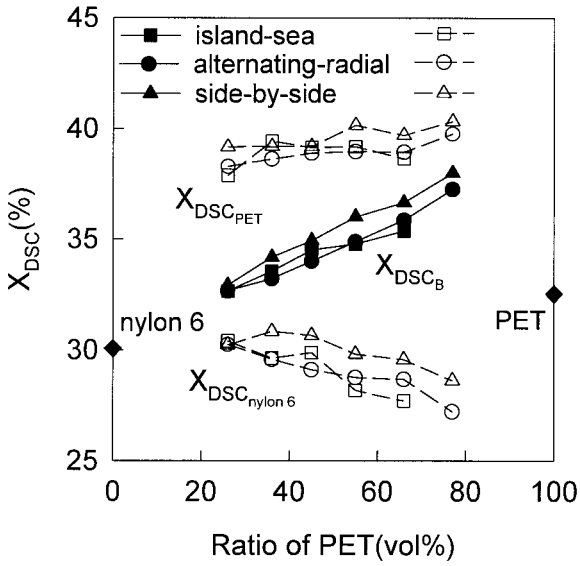

Figure 10 Weight percent crystallinities by DSC of the bicomponent fibers (filled symbols) and each component (blank symbols) in the bicomponent fibers.

10. The crystallinity of the bicomponent fibers by DSC was calculated by Eq. (3), with the data of DSC first heating run:

$$X_{\mathrm{DSC}_B} = w_{\mathrm{PET}} X_{\mathrm{DSC}_{\mathrm{PET}}} + W_{\mathrm{nylon\ 6}} X_{\mathrm{DSC}_{\mathrm{nylon\ 6}}} \qquad (3)$$

where the crystallinity of each component in the bicomponent fibers is:

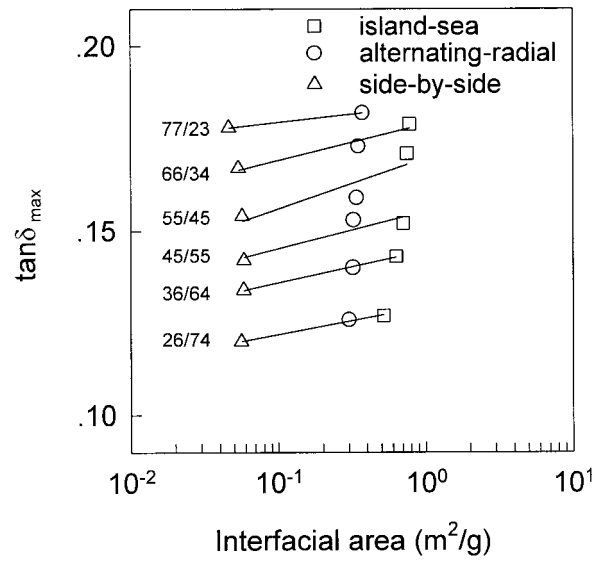

Figure 9 Maximum loss tangent as a function of interfacial area; solid lines: regression lines at the same composition ratios of PET/nylon 6 (vol %).

$$X_{\mathrm{DSC}_x} = (\Delta H_{f_x} - \Delta H_{C_x})/w_x \Delta H^0_{f_x} \qquad (4)$$

where subscript x represents the component, that is, PET or nylon 6 component in the bicomponent fibers, w_x is the weight fraction of the component, ΔH_{f_x} is the heat of fusion of the component, ΔH_{c_x} is the crystallization exotherm of the component, and $\Delta H^0_{f_x}$ is the ideal heat of fusion of the respective homopolymers using the following data; 140 J/g for PET[12] and 230 J/g for nylon 6.[13] In Figure 10, the crystallinities of the bicomponent fibers increase with the increase in the ratio of the PET component, and the side-by-side type bicomponent fiber shows the highest crystallinity among three types of bicomponent fibers at the same composition ratios. Almost all the crystallinities of the bicomponent fibers are higher than those of PET and nylon 6 single-component fibers. Considering the contribution of each component, the crystallinity of the PET component ($X_{\mathrm{DSC}_{\mathrm{PET}}}$) increases slightly with the increase in the ratio of the PET component, but the island-sea type remains almost constant, although the crystallinity of the nylon 6 component ($X_{\mathrm{DSC}_{\mathrm{nylon\ 6}}}$) decreases with the increase in the ratio of PET component. Figure 11 shows the dependence of crystallinity by DSC on the interfacial area of the bicomponent fibers. At the same composition ratios, the crystallinity by DSC increases with the decrease in the interfacial area. Considering the relationship be-

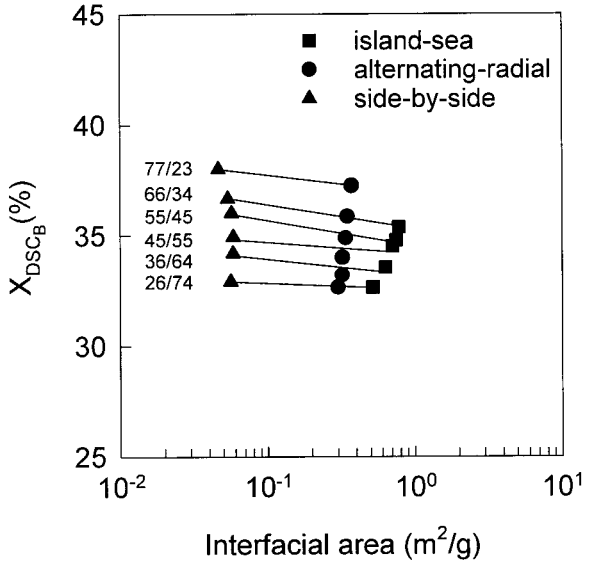

Figure 11 Weight percent crystallinity by DSC of the bicomponent fibers as a function of interfacial area; solid lines: regression lines at the same composition ratios of PET/nylon 6 (vol %).

tween crystallinity and maximum loss tangent, the trend of crystallinity (Fig. 11) is in good agreement with that of the maximum loss tangent (Fig. 9).

Figure 12 shows the WAXS diffraction patterns of the drawn PET/nylon 6 bicomponent fibers at a composition ratio 66/34 (vol %), and the dashed lines are the calculated intensities in proportion to the volume percent of composition, with the intensities of PET and nylon 6 single-component fibers. The crystalline structures of PET component in the bicomponent fibers were improved, but those of nylon 6 component were reduced. From this figure it can be seen that the nylon 6 single-component fiber has the typical diffraction pattern of the γ^* pseudohexagonal crystalline phase[14] and the PET single-component fiber shows immature crystalline structure. The intensities of the bicomponent fibers, compared with the calculated, show the reduced intensity of the characteristic peak of the γ-phase crystalline structure of nylon 6 around 21°, and the improved peaks of PET around 18, 23, and 25°. The qualitative analysis of the diffraction patterns of the bicomponent fibers could give the information on the degree of improvement of the crystalline structure of PET component and simultaneously the degree of reduction of the crystalline structure of nylon 6. As shown in Figure 12, the side-by-side type shows more developed diffraction peak compared with other types of bicomponent fibers, corresponding to (100) lattice plane of PET crystalline structure around 25°. On the contrary, less reduction of diffraction peak corresponding to (010) lattice plane of γ-phase nylon 6 crystalline structure was observed around 21°. It is supposed that the improvement of crystalline structure of the PET component takes place in the bicomponent fiber systems, whereas the imperfect and small crystallites are formed in the vicinity of interfaces. Therefore, the relatively less interface of the side-by-side type contributes to the more improved crystalline structure of PET component in the bicomponent fibers.

The improvement of crystallinity of PET component in the bicomponent fibers, as shown in Figures 10 and 12, was in good agreement with the results of Kikutani et al.[15] and Radhakrishnan et al.[16] Kikutani et al.[15] studied the mechanism of structure development in PET/PP bicomponent fiber systems, and Radhakrishnan et al.[16] studied the low molecular weight PET/high molecular weight PET bicomponent fiber systems. According to their studies on the simple core-sheath type of bicomponent fibers, the structure formation of a component with the higher temperature-dependent elongational viscosity and the higher solidification temperature was expected to

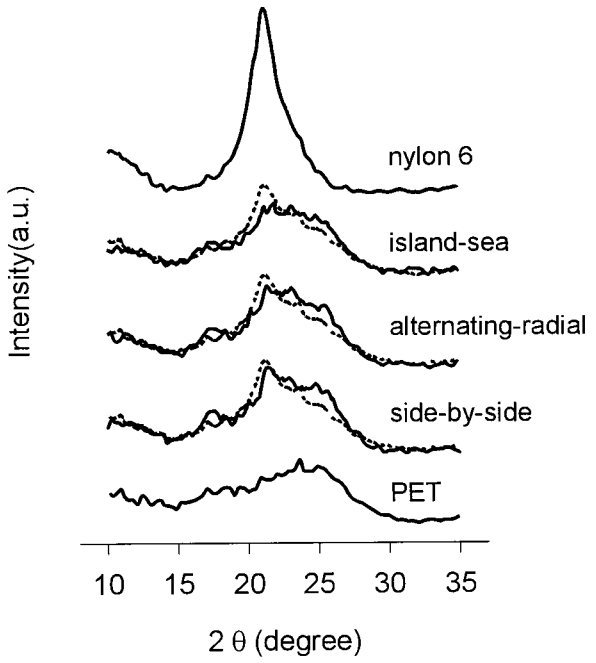

Figure 12 WAXS patterns of the drawn PET/nylon 6 bicomponent fibers at a composition ratio 66/34 vol %; solid lines: observed; dashed lines: calculated with the intensities of single-component PET and nylon 6 fibers.

be enhanced. In this study, PET is the component with the higher temperature-dependent elongational viscosity and the higher solidification temperature. Thus, the crystallinity of PET component was enhanced, and that of nylon 6 component suppressed, and the crystallinity of bicomponent fibers increases with the increase in the PET component, as shown in Figure 10.

In addition to the above statement, it can be concluded that the interfaces between two components in the bicomponent fibers have influence on the crystalline structure and ultimately on the dynamic mechanical properties of PET/nylon 6 bicomponent fibers. As shown in Figures 10 and 12, it is the evidence of these results that the side-by-side type with the smallest interfacial area has the highest crystallinity among three types of bicomponent fibers.

By Murayama and Lawton,[17] the method of the dynamic mechanical test was extended to the dynamic mechanical analysis on the bicomponent system for determining the energy dissipation (loss tangent, tan δ) arising from the poor adhesion. The details of this analysis are shown by Eq. (5):

$$\tan \delta_{adh} = \tan \delta - \tan \delta_B \qquad (5)$$

where tan δ_{adh} is the internal energy dissipation due to the poor adhesion, tan δ is the measured loss tangent for the bicomponent system, and tan δ_B is the loss tangent for the bicomponent system with the assumption of perfect adhesion as in Takayanagi parallel model. The loss tangent (tan δ_B) for the bicomponent system with perfect adhesion is calculated by using Eq. (2). By measuring the total system energy dissipation in terms of tan δ and knowing tan δ_{PET}, tan $\delta_{nylon\ 6}$, and the storage moduli (E'_{PET}, $E'_{nylon\ 6}$) of the components as well as the volume fractions, the internal energy dissipation due to the poor adhesion of interface can be calculated, and it is called the adhesion factor, tan δ_{adh}.[17]

The adhesion factor (tan δ_{adh}) has been applied to the estimation of the effects of interface on the dynamic mechanical properties and the crystalline structure of the bicomponent fibers. The adhesion factors of the bicomponent fibers as a function of the temperature are demonstrated in Figures 13 and 14. The positive values of the adhesion factor mean that the internal energy dissipation of the bicomponent fibers is larger than the calculated prediction with the assumption of perfect adhesion, because of the poor adhesion of interfaces between PET and nylon 6 components, although the negative value of the adhesion factor may be the sign of the decrease of the internal energy dissipation due to the improvement of the crystalline structure of PET/nylon 6 bicomponent fibers. Almost all the adhesion factors have the negative values within the glass transition region of the bicomponent fibers (around 70 to 135°C). The absolute magnitude of the negative adhesion factor means the degree of the improvement of crystalline structure compared with the single components. Figure 13 demonstrates the temperature dependence of the adhesion factor of the side-by-side type of PET/nylon 6 bicomponent fibers. The adhesion factor of the side-by-side type goes through the minimum in the range of 90 to 115°C.

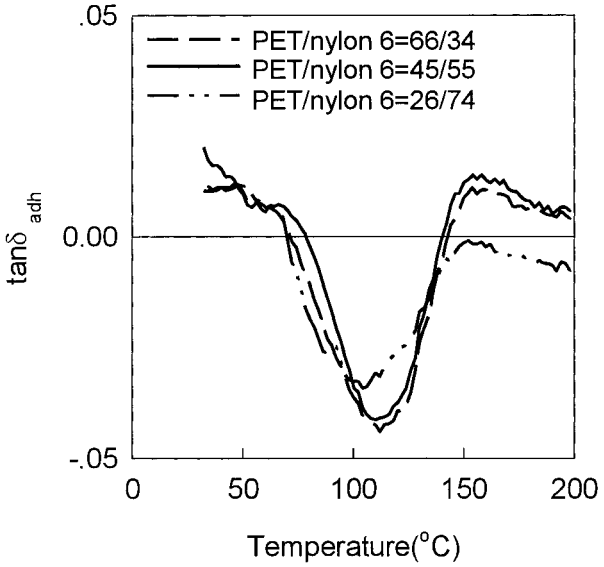

Figure 13 Adhesion factor (tan δ_{adh}) of the side-by-side type of the PET/nylon 6 bicomponent fibers at various composition ratios (vol %).

Figure 14(a) and (b) shows the differences of adhesion factor among the three types of the bicomponent fibers at composition ratios 45/55 and 66/34 vol %, respectively. In both cases, the side-by-side type has the lowest adhesion factor among the three types of bicomponent fibers within the glass transition region (around 70 to 135°C) of the bicomponent fibers and the lowest minimum of the adhesion factor, as shown in Figure 15. This may be caused by the influence of the relatively high crystallinity of side-by-side type. The side-by-side type has the lowest minimum adhesion factor in the whole range of PET composition, and it has good agreement with the trends of maxi-

mum loss tangent (Fig. 7) and crystallinity (Fig. 10).

CONCLUSIONS

The storage moduli of PET/nylon 6 bicomponent fibers are higher, and the maximum values of loss tangent are lower, than the values calculated by the Takayanagi parallel model with perfect adhesion assumption. The side-by-side type of PET/nylon 6 bicomponent fibers with the smallest interfacial area has the lowest maximum loss tangent and the highest crystallinity among the three types of bicomponent fibers at the same composition ratios. With the decrease in interfacial area, the maximum loss tangent decreases and the crystallinity increases at the same composition ratios. It can be concluded that the crystallinity of PET component in the bicomponent fibers is improved, and the degree of improvement is dependent on the interfacial area. Thus, the interface plays an important role in the determination of the dynamic mechanical properties of the bicomponent fibers.

The side-by-side type has the lowest adhesion factor among three types of the bicomponent fibers within the glass transition region (around 70 to 135°C) and the lowest minimum of adhesion factor. Thus, it is possible to apply the adhesion factor to the estimation of the effects of interface on the dynamic mechanical properties and the improvement of crystalline structure of the bicomponent fibers.

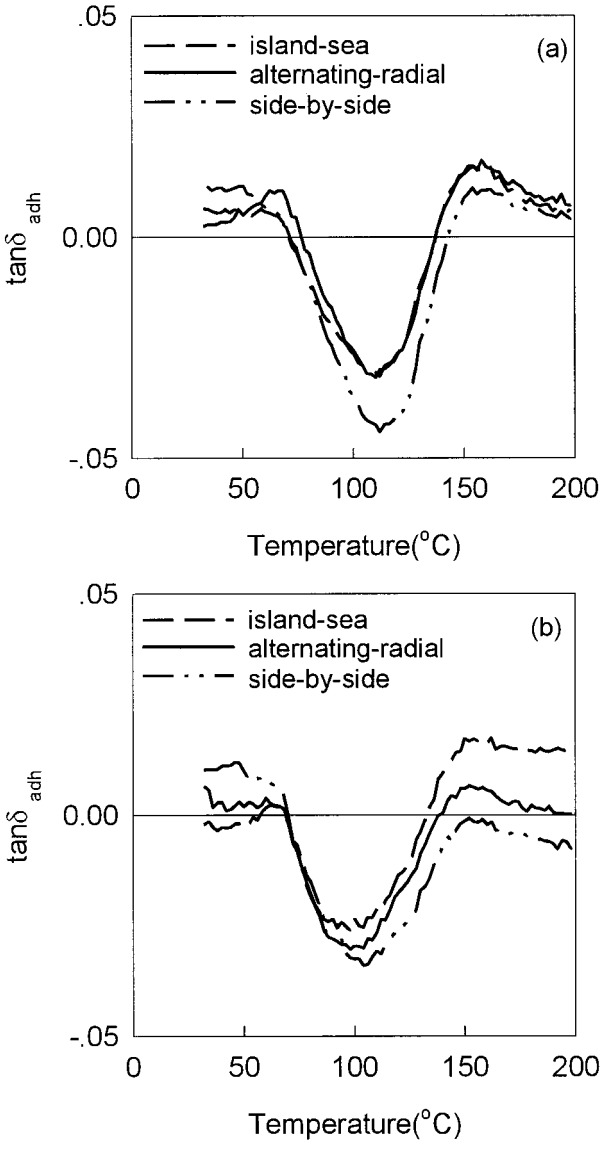

Figure 14 Adhesion factor (tan δ_{adh}) of the PET/nylon 6 bicomponent fibers; (a) at a composition ratio 45/55 vol %; (b) at a composition ratio 66/34 vol %.

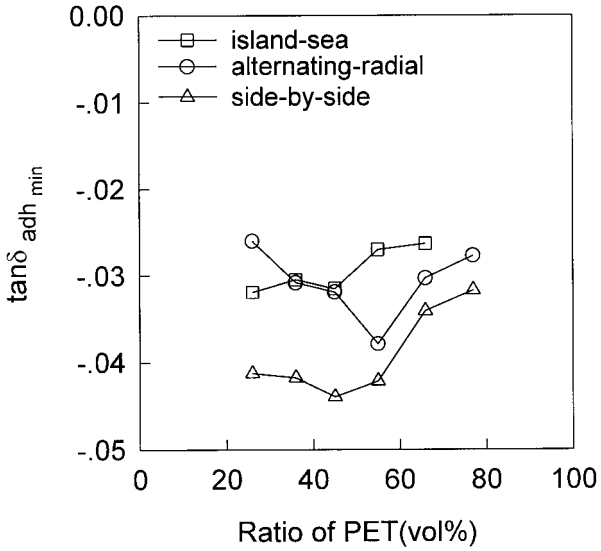

Figure 15 Minimum adhesion factor of the drawn PET/nylon 6 bicomponent.

REFERENCES

1. Hersh, S. P. In Handbook of Fiber Science and Technology, vol. III, High Technology Fibers, Part A; Lewin, M.; Preston, J., Eds.; Marcel Dekker: New York, 1985.
2. Nishimura, M.; Hibino, T.; Tsujimoto, K. Textile Asia 1992, 23, 54.

3. Sperling, L. H. In Recent Advances in Polymer Blends, Grafts and Blocks; Sperling, L. H., Ed.; Plenum Press: New York, 1974, p. 93.
4. Papero, P. V.; Kubu, E.; Roldan, L. Text Res J 1967, 37, 823.
5. Varma, D. S.; Dhar, V. K. J Appl Polym Sci 1987, 33, 1103.
6. Varma, D. S.; Dhar, V. K. Text Res J 1988, 58, 274.
7. Fakirov, S.; Evstatiev, M.; Schultz, J. M. Polymer 1993, 34, 4669.
8. Fukushima, O.; Kogame, K. Sen-I Gakkaishi 1983, 39, P-452.
9. Murayama, T. Dynamic Mechanical Analysis of Polymeric Material; Elsevier Scientific: Amsterdam, 1978.
10. Sperling, L. H. Polymeric Multicomponent Materials; John Wiley & Sons: New York, 1997.
11. Serhatkulu, T.; Erman, B.; Bahar, I.; Fakirov, S.; Evstatiev, M.; Sapundjieva, D. Polymer 1995, 36, 2371.
12. Mehta, A.; Gaur, U.; Wunderich, B. J Polym Sci Polym Phys Ed 1978, 16, 289.
13. Gogolewski, S.; Pennings, A. J. Polymer 1977, 18, 654.
14. Gianchandani, J.; Spruiell, J. E.; Clark, E. S. J Appl Polym Sci 1982, 27, 3527.
15. Kikutani, T.; Radhakrishnan, L.; Arikawa, S.; Takaku, A.; Okui, N.; Jin, X.; Niwa, F.; Kudo, Y. J Appl Polym Sci 1996, 62, 1913.
16. Radhakrishnan, L.; Kikutani, T.; Okui, N. Text Res J 1997, 67, 684.
17. Murayama, T.; Lawton, E. L. J Appl Polym Sci 1973, 17, 669.